



# A high-valent non heme -oxo MnIV dimer generated from a thiolate-bound MnII complex and O<sub>2</sub>

**DOI:**

[10.1002/anie.201703215](https://doi.org/10.1002/anie.201703215)

**Document Version**

Accepted author manuscript

[Link to publication record in Manchester Research Explorer](#)

**Citation for published version (APA):**

Brazzolotto, D., Cantu Reinhard, F., Smith-Jones, J., Retegan, M., Amidani, L., Faponle, A., Ray, K., Philouze, C., De Visser, S., Gennari, M., & Duboc, C. (2017). A high-valent non heme -oxo MnIV dimer generated from a thiolate-bound MnII complex and O<sub>2</sub>. *Angewandte Chemie - International Edition*. <https://doi.org/10.1002/anie.201703215>

**Published in:**

Angewandte Chemie - International Edition

**Citing this paper**

Please note that where the full-text provided on Manchester Research Explorer is the Author Accepted Manuscript or Proof version this may differ from the final Published version. If citing, it is advised that you check and use the publisher's definitive version.

**General rights**

Copyright and moral rights for the publications made accessible in the Research Explorer are retained by the authors and/or other copyright owners and it is a condition of accessing publications that users recognise and abide by the legal requirements associated with these rights.

**Takedown policy**

If you believe that this document breaches copyright please refer to the University of Manchester's Takedown Procedures [<http://man.ac.uk/04Y6Bo>] or contact [uml.scholarlycommunications@manchester.ac.uk](mailto:uml.scholarlycommunications@manchester.ac.uk) providing relevant details, so we can investigate your claim.



## Accepted Article

**Title:** A high-valent non heme  $\mu$ -oxo MnIV dimer generated from a thiolate-bound MnII complex and O<sub>2</sub>

**Authors:** Carole Duboc, Deborah Brazzolotto, Fabián G. Cantú Reinhard, Julian Smith-Jones, Marius Retegan, Lucia Amidani, Abayomi S. Faponle, Kallol Ray, Christian Philouze, Sam P. de Visser, and Marcello Gennari

This manuscript has been accepted after peer review and appears as an Accepted Article online prior to editing, proofing, and formal publication of the final Version of Record (VoR). This work is currently citable by using the Digital Object Identifier (DOI) given below. The VoR will be published online in Early View as soon as possible and may be different to this Accepted Article as a result of editing. Readers should obtain the VoR from the journal website shown below when it is published to ensure accuracy of information. The authors are responsible for the content of this Accepted Article.

**To be cited as:** *Angew. Chem. Int. Ed.* 10.1002/anie.201703215  
*Angew. Chem.* 10.1002/ange.201703215

**Link to VoR:** <http://dx.doi.org/10.1002/anie.201703215>  
<http://dx.doi.org/10.1002/ange.201703215>

# A high-valent non heme $\mu$ -oxo $Mn^{IV}$ dimer generated from a thiolate-bound $Mn^{II}$ complex and $O_2$

Deborah Brazzolotto,<sup>[a,b]</sup> Fabián G. Cantú Reinhard,<sup>[c]</sup> Julian Smith-Jones,<sup>[a]</sup> Marius Retegan,<sup>[d]</sup> Lucia Amidani,<sup>[d]</sup> Abayomi S. Faponle,<sup>[c]</sup> Kallol Ray,<sup>[e]</sup> Christian Philouze,<sup>[a]</sup> Sam P. de Visser,<sup>\*,[c]</sup> Marcello Gennari,<sup>\*,[a]</sup> and Carole Duboc<sup>\*,[a]</sup>

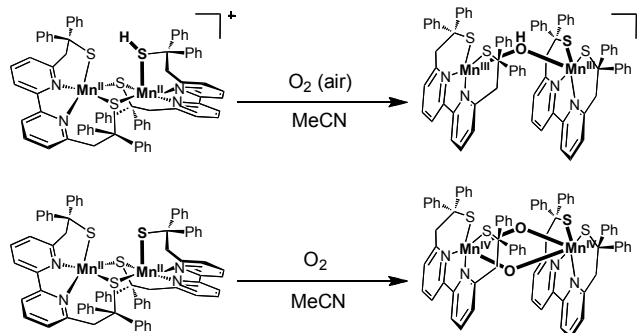
**Abstract:** This study deals with the unprecedented reactivity of dinuclear non heme  $Mn^{II}$ -thiolate complexes with  $O_2$ , which dependent on the protonation state of the initial  $Mn^{II}$  dimer selectively generates either a di- $\mu$ -oxo or  $\mu$ -oxo- $\mu$ -hydroxo  $Mn^{IV}$  complex. Both dimers have been characterized by different techniques including single-crystal X-ray diffraction and mass spectrometry. Oxygenation reactions carried out with labeled  $^{18}O_2$  unambiguously shows that the oxygen atoms present in the  $Mn^{IV}$  dimers originate from  $O_2$ . Based on experimental observations and DFT calculations, evidence is provided that these  $Mn^{IV}$  species compropionate with a  $Mn^{II}$  precursor to yield  $\mu$ -oxo and/or  $\mu$ -hydroxo  $Mn^{III}$  dimers. Our work highlights the delicate balance of reaction conditions to control the synthesis of non heme high-valent  $\mu$ -oxo and  $\mu$ -hydroxo Mn species from  $Mn^{II}$  precursors and  $O_2$ .

Dioxygen activation is critical for all forms of life and fundamental in many biological processes.<sup>[1]</sup> In addition,  $O_2$  is an environmentally benign oxidant in chemical catalysis<sup>[2]</sup> and the development of fuel cells requires electrocatalysts for its efficient and selective reductive activation.<sup>[3]</sup> Activating  $O_2$  often requires transition metal ions to promote the process.<sup>[4]</sup> The detailed understanding of the role of the metal ion and of the mechanism at a molecular level, especially through the characterization of intermediate species, is therefore crucial for the development of efficient catalysts.<sup>[5]</sup> Surprisingly, even though mono- and dinuclear high-valent metal oxo species derived from  $O_2$  have been extensively described for iron<sup>[6]</sup> and copper,<sup>[7]</sup> little is known on the dioxygen chemistry of manganese,<sup>[8]</sup> another cheap and abundant metal. In particular, a non heme oxo  $Mn^{IV}$  complex *directly* generated by reacting  $O_2$  with a  $Mn^{II}$  precursor has yet to be described. Mononuclear oxo and dinuclear  $\mu$ -oxo

$Mn^{IV}$  complexes have been quasi-exclusively generated using oxidizing agents such as  $H_2O_2$ ,  $PhIO$  or peracids.<sup>[8-9]</sup> There is only one case reported by Borovik et al in which the synthesis of an oxo- $Mn^{IV}$  complex derived from  $O_2$  and a  $Mn^{II}$  precursor has been described, but the presence of ferrocenium was required to oxidize the intermediate  $Mn^{III}$  species.<sup>[10]</sup> In a few other studies, oxo- $Mn^{IV}$  species derived from  $O_2$  and a  $Mn^{II}$  complex have been suggested as intermediates but without direct experimental evidence.<sup>[11]</sup> Recently, McKenzie et al evoked the formation of such transient species during the oxidation of benzylic C-H bonds by a  $Mn^{II}$  complex with  $O_2$ .<sup>[11a]</sup> Kovacs et al reported that  $Mn^{II}$  complexes with a thiolate-based supporting ligand activate  $O_2$  through the formation of a *trans*  $\mu$ -1,2-peroxo dinuclear  $Mn^{III}$  complex.<sup>[11b]</sup> This peroxo species directly evolves to a dinuclear  $\mu$ -oxo  $Mn^{III}$  complex implicating the transient formation of oxo  $Mn^{IV}$  species.

In this context, we report here the unprecedented reactivity of a thiolate bound  $Mn^{II}$  complex with  $O_2$  to yield *directly* high valent oxo  $Mn^{IV}$  species. As a precursor the reported dinuclear  $Mn^{II}$  complex  $[Mn^{II}_2(LS)(LSH)]^+$  ( $Mn^{II}_2SH$ ) (with  $LS^{2-} = 2,2'-(2,2'$ -bipyridine-6,6'-diyl)bis(1,1'-diphenylethanethiolate) was used, in which one thiol is terminally bound to a  $Mn^{II}$  ion.<sup>[12]</sup> This complex was previously shown to react with  $O_2$  to generate a hydroxo bridged dinuclear  $Mn^{III}$  complex ( $Mn^{III}_2OH$ ) (Scheme 1, top). In the present work, we provide evidence that the deprotonation of the  $Mn^{II}$ -bound thiol leads to the isolation of the first high-valent oxo  $Mn^{IV}$  dimer *directly* in a reaction with  $O_2$  (Scheme 1, bottom). Finally, a full mechanism of  $O_2$  activation, starting either from  $Mn^{II}_2SH$  or from its deprotonated form  $Mn^{II}_2$ , is proposed based on experimental and computational studies. Especially, we demonstrate that the oxo  $Mn^{IV}$  dimer is an intermediate species for the generation of  $Mn^{III}_2OH$  via compropionate with the initial  $Mn^{II}$  species.

The thiol function of  $Mn^{II}_2SH$  can be deprotonated by addition of NaH (or 2,6-lutidine) to afford  $Mn^{II}_2$ . As expected, deprotonation induces a large decrease of the oxidation potential ( $Mn^{II}Mn^{II}$  to  $Mn^{III}Mn^{III}$ ) of the complex (of  $\sim 300$  mV, see Figure S1).<sup>[12]</sup>



**Scheme 1.** Reaction of  $Mn^{II}_2SH$  (top) and  $Mn^{II}_2$  (down) with  $O_2$  in MeCN at 293 K.

When  $O_2$  is vigorously bubbled through a MeCN solution of  $Mn^{II}_2$ , the colour changes from light brown to black instantaneously

[a] Dr. D. Brazzolotto, Julian Smith-Jones, Dr. C. Philouze, Dr. M. Gennari, Dr. C. Duboc, Univ. Grenoble Alpes, CNRS, UMR 5250, DCM F-38000 Grenoble, France [marcello.gennari@univ-grenoble-alpes.fr](mailto:marcello.gennari@univ-grenoble-alpes.fr), [carole.duboc@univ-grenoble-alpes.fr](mailto:carole.duboc@univ-grenoble-alpes.fr)

[b] Dr. D. Brazzolotto Univ. Grenoble Alpes, CNRS, UMR 5249, LCBM, F-38000 Grenoble, France

[c] F.G. Cantú Reinhard, Dr A.S. Faponle, Dr S.P. de Visser Manchester Institute of Biotechnology and School of Chemical Engineering and Analytical Science The University of Manchester, 131 Princess Street, Manchester M1 7DN, United Kingdom [sam.devisser@manchester.ac.uk](mailto:sam.devisser@manchester.ac.uk)

[d] Dr. M. Retegan, Dr. L. Amidani European Synchrotron Radiation Facility (ESRF) 71 Avenue des Martyrs 38000, Grenoble, France

[e] Prof. Dr.K.Ray Department of Chemistry, Humboldt-Universität zu Berlin Brook-Taylor-Strasse2, 12489 Berlin (Germany)

Supporting information for this article is given via a link at the end of the document.

with the appearance of a weak absorption band at 560 nm (Figure S2) that is assigned to the di- $\mu$ -oxo  $\text{Mn}^{\text{IV}}$  dimer,  $\text{Mn}^{\text{IV}}_2(\text{O})_2$ . The conversion is quantitative based on the UV-vis spectrum of the oxygenated solution. Its structure, resolved by single crystal X-ray crystallography, displays a perfect planar  $\{\text{Mn}_2\text{O}_2\}$  core with a  $C_2$  symmetry axis passing through the two O atoms with each Mn in the center of a distorted  $\text{N}_2\text{S}_2\text{O}_2$  octahedron (Figure 1a). The Mn $\cdots$ Mn distance (2.7821(16) Å) and the Mn-O-Mn angles (100.5(2)° and 97.84(19)°) are consistent with a di- $\mu$ -oxo  $\text{Mn}^{\text{IV}}$  complex, where typical values in the range of 2.672–2.757 Å and 95.2–101.5° are found, respectively.<sup>[13]</sup>

X-ray absorption spectroscopy (XAS, Figure S3) and electrospray ionization (ESI)-mass spectrometry (Figures 2, S4, and S5) reveal the retention of the  $\text{Mn}^{\text{IV}}_2(\text{O})_2$  structure in solution. The Mn K-edge absorption spectrum of  $\text{Mn}^{\text{IV}}_2(\text{O})_2$  shows a shift to higher energy (6547.4 eV) of the Mn(1s)  $\rightarrow$  Mn(4p) transition with respect to  $\text{Mn}^{\text{II}}_2\text{SH}$  and  $\text{Mn}^{\text{II}}_2\text{OH}$  (6545.5 and 6546.2 eV, respectively), as evidence of a +IV oxidation state for both Mn ions (Figure 3). The mass spectrum of a MeCN solution of  $\text{Mn}^{\text{IV}}_2(\text{O})_2$  ( $m/z = 1299.4$ ) indicates the presence of two additional oxygen atoms compared to the initial  $\text{Mn}^{\text{II}}_2$  complex ( $m/z = 1267.3$ ). Furthermore, when  $\text{Mn}^{\text{IV}}_2(\text{O})_2$  is generated in the presence of labeled  $^{18}\text{O}_2$ , only the  $\text{Mn}^{\text{IV}}_2(^{18}\text{O})_2$  complex is observed in the mass spectrum ( $m/z = 1303.3$ ). The present study unambiguously demonstrates that one molecule of  $\text{O}_2$  reacts with  $\text{Mn}^{\text{II}}_2$  to form the two oxo-bridges in  $\text{Mn}^{\text{IV}}_2(\text{O})_2$ . To the best of our knowledge, this is the first report on a  $\text{Mn}^{\text{II}}$  complex able to directly activate molecular oxygen to form a high-valent oxo- $\text{Mn}^{\text{IV}}$  species.

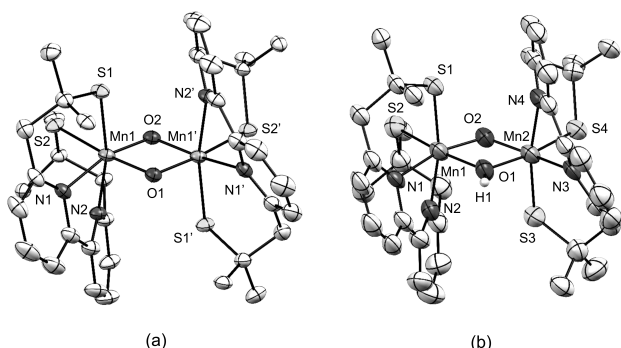


**Figure 1.** Molecular structures of (a)  $\text{Mn}^{\text{IV}}_2(\text{O})_2 \cdot 1.34\text{CH}_2\text{Cl}_2 \cdot 5.82\text{H}_2\text{O}$  and (b)  $\text{Mn}^{\text{IV}}_2(\text{O})(\text{OH})\text{ClO}_4 \cdot 5.68\text{CH}_3\text{CN} \cdot 1.5\text{H}_2\text{O}$ . The thermal ellipsoids are drawn at 50% probability level. For clarity, phenyl groups, all hydrogen atoms (except for H1 in b), anions and solvent molecules are omitted. Selected bond distances (Å): in  $\text{Mn}^{\text{IV}}_2(\text{O})_2$ , Mn1–O1 = 1.845(3), Mn1–O2 = 1.809(3), Mn1–Mn1' = 2.7821(16); in  $\text{Mn}^{\text{IV}}_2(\text{O})(\text{OH})$ , Mn1–O1 = 1.959(6), Mn1–O2 = 1.819(6), Mn1–Mn1' = 2.922(2).

The acid-base properties of  $\text{Mn}^{\text{IV}}_2(\text{O})_2$  were investigated by UV-vis absorption spectroscopy in dimethylformamide solution at 273 K. In the presence of 1 equiv. of  $\text{HClO}_4$ , the 560 nm transition, characteristic for  $\text{Mn}^{\text{IV}}_2(\text{O})_2$ , disappears with the concomitant apparition of two weak bands at 520 nm and 680 nm assigned to  $\text{Mn}^{\text{IV}}_2(\text{O})(\text{OH})$  (see Figure S2). The subsequent addition of 1 equiv. of a strong base (tBuOK) restores the initial

UV-vis spectrum with a loss of about 10% of the intensity due to the slow decomposition of the complex in solution. Consistently no EPR transition could be observed in their respective spectra since an antiferromagnetic coupling between the two  $\text{Mn}^{\text{IV}}$  ions is expected resulting in a total spin  $S = 0$  in both complexes.

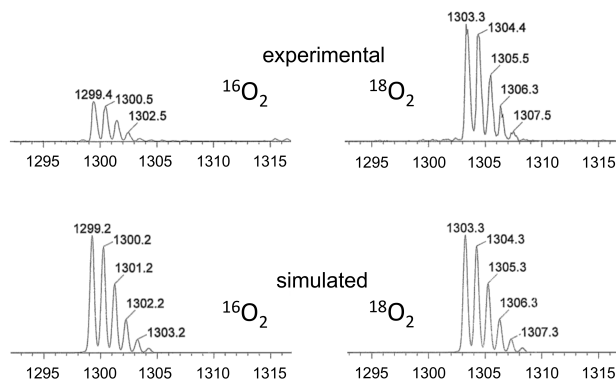


**Figure 2.** Experimental and simulated ESI-mass spectra of  $\text{Mn}^{\text{IV}}_2(\text{O})_2$  generated from  $\text{Mn}^{\text{II}}_2$  and either  $^{16}\text{O}_2$  or  $^{18}\text{O}_2$ .

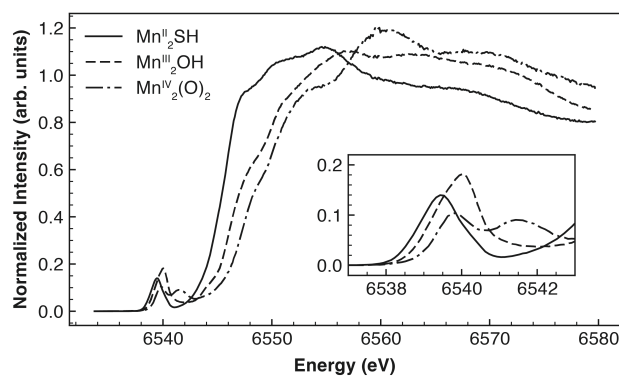


**Figure 3.** (a) Mn K-edge XAS spectra recorded on powdered samples of  $\text{Mn}^{\text{II}}_2$ ,  $\text{Mn}^{\text{II}}_2\text{OH}$ , and  $\text{Mn}^{\text{IV}}_2(\text{O})_2$ . The pre-edge region is shown in the inset.

The formed protonated species was assigned to a dinuclear  $\mu$ -oxo- $\mu$ -hydroxo  $\text{Mn}^{\text{IV}}$  complex,  $\text{Mn}^{\text{IV}}_2(\text{O})(\text{OH})$ , based on the structure resolved by single crystal X-ray diffraction (Figure 1b). It represents the first crystallographically characterized  $\mu$ -oxo- $\mu$ -hydroxo dinuclear  $\text{Mn}^{\text{IV}}$  complex in the literature. Previously, Pecoraro et al. reported a series of di- $\mu$ -oxo,  $\mu$ -oxo- $\mu$ -hydroxo, di- $\mu$ -hydroxo dinuclear  $\text{Mn}^{\text{IV}}$  complexes obtained with the salpn ligand (salpn = *N,N'*-bis(salicylidene)-1,3-diaminopropane). However, they only managed to structurally characterize these compounds by extended X-ray absorption fine structure (EXAFS) spectroscopy (except for the  $[\text{Mn}^{\text{IV}}_2(\text{salpn})_2(\mu\text{-O})_2]$  complex).<sup>[14]</sup> The  $\{\text{Mn}_2\text{O}_2\}$  core of  $\text{Mn}^{\text{IV}}_2(\text{O})(\text{OH})$  is planar as in  $\text{Mn}^{\text{IV}}_2(\text{O})_2$ . In  $\text{Mn}^{\text{IV}}_2(\text{O})(\text{OH})$ , the two Mn sites are not equivalent anymore and each Mn centre has a distorted  $\text{N}_2\text{S}_2(\text{O})(\text{OH})$  octahedral geometry. In agreement with the presence of a hydroxo bridge, the Mn-O1(H) distance is about 10 pm longer (1.959(6) Å) than the Mn-O2 one (1.819(6) Å). Coherently, the

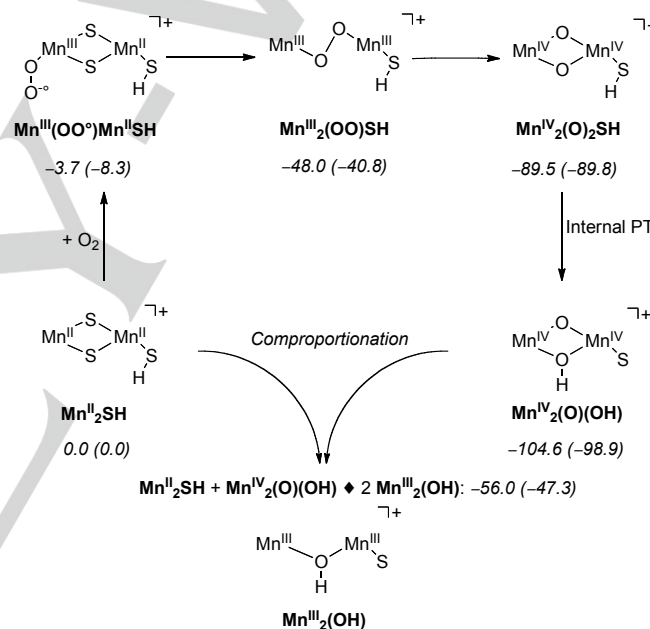
Mn<sup>III</sup>-Mn distance in **Mn<sup>IV</sup><sub>2</sub>(O)(OH)** (2.922(2) Å) is longer than in **Mn<sup>IV</sup><sub>2</sub>(O)<sub>2</sub>** (2.7821(16) Å). The presence of the hydroxo bridge leads also to a smaller Mn1-O1(H)-Mn2 angle (96.1(3)°) with respect to the Mn1-O2-Mn2 one (107.2(3)°). The structural features of the Mn-O and Mn-O(H) bonds in **Mn<sup>IV</sup><sub>2</sub>(O)<sub>2</sub>** and **Mn<sup>IV</sup><sub>2</sub>(O)(OH)** are similar to those found by Pecoraro et al.<sup>[14b]</sup> Subsequently, we evidenced that these high-valent oxo Mn<sup>IV</sup> compounds are also involved as intermediates in the O<sub>2</sub> activation by the protonated **Mn<sup>II</sup><sub>2</sub>SH** precursor. Firstly, we observed that this process can be directed towards either **Mn<sup>IV</sup><sub>2</sub>(O)(OH)** or **Mn<sup>III</sup><sub>2</sub>OH** by tuning the experimental conditions (relative concentration between the Mn<sup>II</sup> precursor and O<sub>2</sub>, protonation state of the Mn<sup>II</sup> complex, temperature). Secondly, with the support of UV-vis absorption spectroscopy and ESI-mass spectrometry, we have made the following key observations: (i) even if both **Mn<sup>IV</sup><sub>2</sub>(O)(OH)** and **Mn<sup>IV</sup><sub>2</sub>(O)<sub>2</sub>** decompose over time, none can directly evolve to **Mn<sup>III</sup><sub>2</sub>OH** or to its deprotonated form **Mn<sup>III</sup><sub>2</sub>O**, i.e. the μ-oxo Mn<sup>III</sup> dimer,<sup>[15]</sup> (ii) **Mn<sup>IV</sup><sub>2</sub>(O)<sub>2</sub>** reacts instantaneously with **Mn<sup>II</sup><sub>2</sub>SH** or **Mn<sup>II</sup><sub>2</sub>** to generate **Mn<sup>III</sup><sub>2</sub>OH** and/or **Mn<sup>III</sup><sub>2</sub>O** via a comproportionation reaction, and (iii) the latter process is more efficient when the Mn<sup>II</sup> precursor is protonated, i.e. **Mn<sup>II</sup><sub>2</sub>SH**.

In the absence of available kinetic data (the oxygenation process is diffusion-limited), we have performed a DFT study to better understand the difference in reactivity between **Mn<sup>II</sup><sub>2</sub>SH** and **Mn<sup>II</sup><sub>2</sub>**. These exploratory calculations on the possible reaction cycles have been performed using previously benchmarked and calibrated methods for biomimetic manganese complexes.<sup>[16]</sup> The overall mechanism proposed for the reaction of **Mn<sup>II</sup><sub>2</sub>SH** with O<sub>2</sub> is reported in Scheme 2 (see also Schemes S1 and S2) with a simplified representation of all calculated intermediate species. The activation of O<sub>2</sub> is proposed to go through the formation of a dinuclear *trans*-μ-1,2-peroxy Mn<sup>III</sup> complex, **Mn<sup>III</sup><sub>2</sub>(OO)SH**, whose calculated structural parameters are comparable to those reported for the similar complex described by Kovacs et al.<sup>[11b]</sup> This *trans*-μ-1,2-peroxy Mn<sup>III</sup> complex converts to a dinuclear di-μ-oxo Mn<sup>IV</sup> species with large exothermicity (of -41.5 kcal mol<sup>-1</sup>), and a low transition state (**TS<sub>OO</sub>**) with a barrier of only 5.8 kcal mol<sup>-1</sup>. The rupture of the O-O bond leads to a rapid internal proton transfer from the thiol to one of the bridging oxygen atoms via a proton transfer barrier (**TS<sub>PT</sub>**) of about 11.5 kcal mol<sup>-1</sup> and the formation of the experimentally characterized **Mn<sup>IV</sup><sub>2</sub>(O)(OH)** complex. Then a comproportionation reaction with a molecule of **Mn<sup>II</sup><sub>2</sub>SH** can occur to form the dinuclear μ-hydroxo Mn<sup>III</sup> product, **Mn<sup>III</sup><sub>2</sub>OH**, with large exothermicity (-56.0 kcal mol<sup>-1</sup>). As each individual step in the reaction mechanism of Scheme 2 is exothermic, this implies that the reaction is irreversible and the final products will be the most stable. As a matter of fact, most of these structures could be characterized experimentally, hence validating our proposed mechanism.

We have also calculated the mechanism of O<sub>2</sub> activation starting from the deprotonated **Mn<sup>II</sup><sub>2</sub>** complex (Scheme S2 and Figure S6). It is found that the process is energetically less favorable than the one starting from the **Mn<sup>II</sup><sub>2</sub>SH** complex, but still feasible. From these different pathways, it can be concluded that the formation of either a dinuclear Mn<sup>III</sup> or Mn<sup>IV</sup> complex will depend on the relative rates between the O<sub>2</sub> activation processes (steps 1-2 in Scheme 2, formation of **Mn<sup>III</sup><sub>2</sub>(OO)SH**) and the

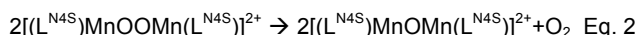
comproportionation reaction (step 5 in Scheme 2). In the case of a faster O<sub>2</sub> activation, the initial Mn<sup>II</sup> complex will be entirely consumed to form the Mn<sup>IV</sup> derivative and thus the Mn<sup>III</sup> dimer cannot be generated. Conversely, in the case of a faster comproportionation reaction, a part of the Mn<sup>II</sup> complex will remain unreacted to O<sub>2</sub>, and will thus combine with the generated Mn<sup>IV</sup> species to yield the Mn<sup>III</sup> dimer. This is consistent with the fact that a higher concentration of O<sub>2</sub> vs. Mn<sup>II</sup> complex promotes the formation of the Mn<sup>IV</sup> compound as final product instead of **Mn<sup>III</sup><sub>2</sub>OH**.

Based on these considerations, two complementary reasons can explain how protonation of the Mn<sup>II</sup> precursor favors the production of the Mn<sup>III</sup> complex to the detriment of the Mn<sup>IV</sup> one: (i) O<sub>2</sub> activation is expected to be slower in the case of **Mn<sup>II</sup><sub>2</sub>SH** (higher Mn<sup>II,III</sup>/Mn<sup>II,III</sup> anodic potential compared to **Mn<sup>II</sup><sub>2</sub>**) and (ii) the comproportionation reaction is more efficient when protonated species are involved, as shown experimentally (see above) and corroborated by DFT.



**Scheme 2.** Dioxygen activation mechanism on **Mn<sup>II</sup><sub>2</sub>SH** as calculated using DFT at the BLYP/BS2//BLYP/BS1 level of theory. Relative energies of the antiferromagnetic spin states for the pathway leading to the **Mn<sup>IV</sup><sub>2</sub>(O)(OH)** complex are in kcal mol<sup>-1</sup> with respect to **Mn<sup>II</sup><sub>2</sub>SH** + O<sub>2</sub> and contain zero-point energy and solvent corrections. Data out of parenthesis represent the full model and inside parenthesis the small model with methyl rather than phenyl substituents on the N2S2 ligand. Also given are the energetics for the comproportionation reaction.

The calculated mechanism reveals a short-lived *trans* μ-1,2 peroxy Mn<sup>III</sup> complex as a key intermediate in the formation of high valent oxo/hydroxo Mn<sup>III</sup> and Mn<sup>IV</sup> dimers from the reaction of the Mn<sup>II</sup> complexes with O<sub>2</sub> (Table S23). As noted previously, a similar peroxy complex has been isolated by the Kovacs group through the reaction of a Mn<sup>II</sup> thiolate complex ([Mn(L<sup>N4S</sup>)<sup>+</sup>] with O<sub>2</sub>, and characterized by single crystal X-ray diffraction (Scheme S3). This complex slowly evolves into a dinuclear μ-oxo Mn<sup>III</sup> complex (Eqs 1 and 2).<sup>[11b]</sup>



Although  $\text{Mn}^{\text{II}}_2$  (or  $\text{Mn}^{\text{II}}_2\text{SH}$ ) and  $[\text{Mn}(\text{L}^{\text{N4S}})]^{+}$  complexes contain a thiolate-based ligand, their reactivity patterns are significantly different. First, in the Kovacs' system the peroxy  $\text{Mn}^{\text{III}}$  species is the most stable intermediate, while in our case it is the di- $\mu$ -oxo  $\text{Mn}^{\text{IV}}$  species (the peroxy intermediate is too reactive to be trapped). Secondly, to form the dinuclear  $\mu$ -oxo  $\text{Mn}^{\text{III}}$  complex, a comproportionation reaction is required with the  $\text{LS}^{2-}$  system, while the Kovacs' peroxy,  $[(\text{L}^{\text{N4S}})\text{MnOOMn}(\text{L}^{\text{N4S}})]^{2+}$ , evolves directly into the  $[(\text{L}^{\text{N4S}})\text{MnOMn}(\text{L}^{\text{N4S}})]^{2+}$  species (Eq. 2).

In principle, this "direct" pathway should also be considered for  $\text{Mn}^{\text{III}}_2(\text{OO})\text{SH}$ , but this reaction does not occur as observed experimentally in solution. Although the hypothetical dissociation of two  $\text{Mn}^{\text{III}}_2(\text{OO})\text{SH}$  complexes into two  $\text{Mn}^{\text{III}}_2\text{OH}$  complexes and  $\text{O}_2$  (as in Eq. 2) should be preferred under thermodynamic control (the calculated energy gap of  $-64.6 \text{ kcal mol}^{-1}$  is larger than that between  $\text{Mn}^{\text{III}}_2(\text{OO})\text{SH}$  and  $\text{Mn}^{\text{IV}}_2(\text{O})_2\text{SH}$ , which is of  $-41.5 \text{ kcal mol}^{-1}$ ), the lifetime of  $\text{Mn}^{\text{III}}_2(\text{OO})\text{SH}$  is too short to allow the reaction with a second  $\text{Mn}^{\text{III}}_2(\text{OO})\text{SH}$  molecule and the peroxy species more readily evolves into  $\text{Mn}^{\text{IV}}_2(\text{O})(\text{OH})$ . Such difference in reactivity between our system and the one of Kovacs et al. is consistent with the fact that the O-O bond is longer in the calculated structure of  $\text{Mn}^{\text{III}}_2(\text{OO})\text{SH}$  than in  $[(\text{L}^{\text{N4S}})\text{MnOOMn}(\text{L}^{\text{N4S}})]^{2+}$  ( $1.488 \text{ \AA}$  vs  $1.452 \text{ \AA}$ , respectively). Indeed DFT shows that the O-O bond is more easily cleaved in  $\text{Mn}^{\text{III}}_2(\text{OO})\text{SH}$ . The lower stability of  $\text{Mn}^{\text{III}}_2(\text{OO})\text{SH}$  compared to  $[(\text{L}^{\text{N4S}})\text{MnOOMn}(\text{L}^{\text{N4S}})]^{2+}$  may be also rationalized in terms of differences in metal coordination sphere. First, the N2S2 ligand leads to a peroxy dimer with an unfavorable 5-coordinated geometry for a Jahn-Teller  $\text{Mn}^{\text{III}}$  ion, while a stable peroxy  $\text{Mn}^{\text{III}}$  dimer with a suited 6-coordinated geometry is obtained with the  $\text{L}^{\text{N4S}}$  ligand. Secondly, the O-O bond cleavage of  $\text{Mn}^{\text{III}}_2(\text{OO})\text{SH}$  yields a stable 6-coordinated di- $\mu$ -oxo  $\text{Mn}^{\text{IV}}$  species, while formation of a similar species with the  $\text{L}^{\text{N4S}}$  ligand features is unlikely since it should involve the formation of a 7-coordinated  $\text{Mn}^{\text{IV}}$  complex or the decoordination of a N-based donor atom.

Although the reactivity of these two thiolate-based  $\text{Mn}^{\text{III}}$  complexes differs significantly, the role of the metal-bound thiolate to promote  $\text{O}_2$  activation is, however, once more highlighted.

In summary, our work reports the unprecedented generation of non heme  $\mu$ -oxo  $\text{Mn}^{\text{IV}}$  complexes from the reaction between thiolate  $\text{Mn}^{\text{III}}$  complexes with  $\text{O}_2$ . We showed that, by conveniently tuning the experimental conditions (room temperature, ligand deprotonation, low precursor concentration and high  $\text{O}_2$  concentration), the process can be directed to fully-characterized high-valent  $\mu$ -oxo and  $\mu$ -hydroxo- $\mu$ -oxo  $\text{Mn}^{\text{IV}}$  dimers.

## Acknowledgements

The authors gratefully acknowledge research support of this work by the French National Agency for Research (no. ANR-09-JCJC-0087), Labex arcane (ANR-11-LABX-003) and COST Action (CM1305 ECOSTBio, Explicit Control Over Spin-States in Technology and Biochemistry) especially via STSM 34962. FGCR and ASF thank the Conacyt Mexico and the Tertiary Education Trust Fund Nigeria for studentships, respectively. XAS studies at SSRL BL 9-3 were made possible by the US DOE Office of Science (Contract No. DE-AC02-76SF00515) and US NIH (P41-GM-103393 to SSRL SMB Program and P30-EB-009998 to CWRU Center for Synchrotron Biosciences. We thank Dr. E. W. Farquhar for collection of data. The European Synchrotron Radiation Facility (ESRF) is acknowledged for providing beam time on ID26 and for technical support.

**Keywords:**  $\text{O}_2$  activation • manganese • thiolate • high valent oxo species • mechanistic studies

- [1] a) L. I. Simandi, *Advances in Catalytic Activation of Dioxygen by Metal Complexes*. [In: *Catal. Met. Complexes 2003*; 26], Kluwer Academic Publishers, **2003**; b) V. R. I. Kaila, M. I. Verkhovskiy, M. Wikstrom, *Chem. Rev.* **2010**, *110*, 7062-7081; c) W. B. Tolman, E. I. Solomon, *Inorg. Chem.* **2010**, *49*, 3555-3556; d) S. Hematian, I. Garcia-Bosch, K. D. Karlin, *Acc. Chem. Res.* **2015**, *48*, 2462-2474
- [2] A. E. Shilov, G. B. Shul'pin, *Chem. Rev.* **1997**, *97*, 2879-2932.
- [3] a) S. B. Adler, *Chem. Rev.* **2004**, *104*, 4791-4843; b) M. Shao, Q. Chang, J.-P. Dodelet, R. Chenitz, *Chem. Rev.* **2016**, *116*, 3594-3657.
- [4] a) G. M. Yee, W. B. Tolman, in *Sustaining Life on Planet Earth: Metalloenzymes Mastering Dioxygen and Other Chewy Gases* (Eds.: P. M. H. Kroneck, M. E. Sosa Torres) Springer International Publishing, Cham, **2015**, pp. 131-204; b) A. T. Fiedler, A. A. Fischer, *J. Biol. Inorg. Chem.* **2016**, doi: 10.1007/s00775-00016-01402-00777.
- [5] a) S. Fukuzumi, K. Okamoto, C. P. Gros, R. Guillard, *J. Am. Chem. Soc.* **2004**, *126*, 10441-10449; b) Z. Halime, H. Kotani, Y. Li, S. Fukuzumi, K. D. Karlin, *Proc. Natl. Acad. Sci. U. S. A.* **2011**, *108*, 13990-13994; c) L. Tahsini, H. Kotani, Y.-M. Lee, J. Cho, W. Nam, K. D. Karlin, S. Fukuzumi, *Chem. Eur. J.* **2012**, *18*, 1084-1093; d) K. Ray, F. F. Pfaff, B. Wang, W. Nam, *J. Am. Chem. Soc.* **2014**, *136*, 13942-13958; e) J. Rosenthal, D. G. Nocera, *Acc. Chem. Res.* **2007**, *40*, 543-553; f) M. Costas, M. P. Mehn, M. P. Jensen, L. Que Jr, *Chem. Rev.* **2004**, *104*, 939-986; g) P. Peljo, L. Murtomaki, T. Kallio, H.-J. Xu, M. Meyer, C. P. Gros, J.-M. Barbe, H. H. Girault, K. Laasonen, K. Kontturi, *J. Am. Chem. Soc.* **2012**, *134*, 5974-5984.
- [6] a) E. I. Solomon, S. Goudarzi, K. D. Sutherlin, *Biochemistry* **2016**, *55*, 6363-6374; b) W. Nam, *Acc. Chem. Res.* **2015**, *48*, 2415-2423; c) A. R. McDonald, L. Que Jr, *Coord. Chem. Rev.* **2013**, *257*, 414-428.
- [7] a) E. I. Solomon, *Inorg. Chem.* **2016**, *55*, 6364-6375; b) D. A. Quist, D. E. Diaz, J. J. Liu, K. D. Karlin, *J. Biol. Inorg. Chem.* **2017**, *22*, 253-288; c) W. Keown, J. B. Gary, T. D. P. Stack, *J. Biol. Inorg. Chem.* **2017**, *22*, 289-306; d) S. D. McCann, S. S. Stahl, *Acc. Chem. Res.* **2015**, *48*, 1756-1766; e) C. E. Elwell, N. L. Gagnon, B. D. Neisen, D. Dhar, A. D. Spaeth, G. M. Yee, W. B. Tolman, *Chem. Rev.* **2017**, *117*, 2059-2107.
- [8] S. Sahu, D. P. Goldberg, *J. Am. Chem. Soc.* **2016**, *138*, 11410-11428.
- [9] X. Engelmann, I. Monte-Pérez, K. Ray, *Angew. Chem. Int. Ed.* **2016**, *55*, 7632-7649.
- [10] T. H. Parsell, R. K. Behan, M. T. Green, M. P. Hendrich, A. S. Borovik, *J. Am. Chem. Soc.* **2006**, *128*, 8728-8729.

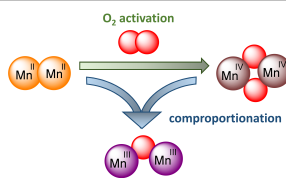
- [11] a) C. Deville, S. K. Padamati, J. Sundberg, V. McKee, W. R. Browne, C. J. McKenzie, *Angew. Chem. Int. Ed.* **2016**, *55*, 545-549; b) M. K. Coggins, X. Sun, Y. Kwak, E. I. Solomon, E. V. Rybak-Akimova, J. A. Kovacs, *J. Am. Chem. Soc.* **2013**, *135*, 5631-5640.
- [12] M. Gennari, D. Brazzolotto, J. Pecaut, M. V. Cherrier, C. J. Pollock, S. DeBeer, M. Retegan, D. A. Pantazis, F. Neese, M. Rouzieres, R. Clerac, C. Duboc, *J. Am. Chem. Soc.* **2015**, *137*, 8644-8653.
- [13] S. Mukhopadhyay, S. K. Mandal, S. Bhaduri, W. H. Armstrong, *Chem. Rev.* **2004**, *104*, 3981-4026.
- [14] a) M. J. Baldwin, T. L. Stemmler, P. J. Riggs-Gelasco, M. L. Kirk, J. E. Penner-Hahn, V. L. Pecoraro, *J. Am. Chem. Soc.* **1994**, *116*, 11349-11356; b) V. Krewald, B. Lassalle-Kaiser, T. T. Boron, C. J. Pollock, J. Kern, M. A. Beckwith, V. K. Yachandra, V. L. Pecoraro, J. Yano, F. Neese, S. DeBeer, *Inorg. Chem.* **2013**, *52*, 12904-12914.
- [15] **Mn<sup>III</sup><sub>2</sub>(OH)** and **Mn<sup>III</sup><sub>2</sub>(OH)** cannot be distinguished by UV-visible spectroscopy since both spectra are dominated by one intense thiolate to Mn<sup>III</sup> charge transfer feature.
- [16] a) T. Yang, M. G. Quesne, H. M. Neu, F. G. Cantú Reinhard, D. P. Goldberg, S. P. de Visser, *J. Am. Chem. Soc.* **2016**, *138*, 12375-12386; b) P. Barman, P. Upadhyay, A. S. Faponle, J. Kumar, S. S. Nag, D. Kumar, C. V. Sastri, S. P. de Visser, *Angew. Chem. Int. Ed.* **2016**, *55*, 11091-11095.

Entry for the Table of Contents (Please choose one layout)

Layout 1:

## COMMUNICATION

**Thiolate is the key.** Dinuclear  $Mn^{II}$ -thiolate complexes display an unprecedented reactivity: direct  $O_2$  activation to generate dinuclear high-valent oxo Mn species, including a di- $\mu$ -oxo  $Mn(IV)$  dimer. Depending on the experimental conditions, the nature of the oxidized Mn species is different. A mechanism based on theoretical calculations is discussed to rationalize all experimental data.



Deborah Brazzolotto, Fabián G. Cantú Reinhard, Julian Smith-Jones, Marius Retegan, Abayomi S. Faponle, Kallol Ray, Christian Philouze, Sam P. de Visser,\* Marcello Gennari,<sup>†</sup> and Carole Duboc\*

Page No. – Page No.

**A high-valent non heme  $\mu$ -oxo  $Mn^{IV}$  dimer generated from a thiolate-bound  $Mn^{II}$  complex and  $O_2$**

Accepted Manuscript